

## LYMPHOID NEOPLASIA

## Eradication of non-Hodgkin lymphoma through the induction of tumor-specific T-cell immunity by CD20-Flex BiFP

Lei Zhao,<sup>1-3</sup> Qin Tong,<sup>1</sup> Weizhu Qian,<sup>1,3</sup> Bohua Li,<sup>1</sup> Dapeng Zhang,<sup>1,3</sup> Tuo Fu,<sup>4</sup> Shuyan Duan,<sup>5</sup> Xueguang Zhang,<sup>4</sup> Jian Zhao,<sup>1-3</sup> Jianxin Dai,<sup>1-3</sup> Hao Wang,<sup>1-3</sup> Sheng Hou,<sup>1-3</sup> and Yajun Guo<sup>1-5</sup>

<sup>1</sup>International Joint Cancer Institute, Second Military Medical University, Shanghai, People's Republic of China; <sup>2</sup>PLA General Hospital Cancer Center, PLA School of Medicine, Beijing, People's Republic of China; <sup>3</sup>The State Key Laboratory of Antibody Medicine and Targeting Therapy and Shanghai Key Laboratory of Cell Engineering and Antibody, Shanghai, People's Republic of China; <sup>4</sup>Institute of Medical Biotechnology, Soochow University, Suzhou, People's Republic of China; and <sup>5</sup>School of Pharmaceutical, Liaocheng University, Liaocheng, Shandong, People's Republic of China

## Key Points

- Targeting of both CD20 and Flt3 proteins by CrossMab technology can efficiently evoke tumor-specific T-cell immunity.
- Induction of tumor-specific T-cell response by CD20–Flt3 ligand extracellular domain BiFP provides a long-lasting protection from tumor recurrence.

Although monoclonal antibodies, including CD20 antibody rituximab, are standard therapeutics for several cancers, their efficacy remains variable and often modest. There is an urgent need to enhance the efficacy of the current generation of anticancer antibodies. Flt3 ligand, a soluble protein, has the ability to induce substantial expansion of dendritic cells (DCs). In this study, we constructed a bispecific immunoglobulin G-like bispecific fusion protein (BiFP) targeting both CD20 and Flt3 (CD20-Flex) by using CrossMab technology. We found that the BiFP exhibited stabilities that were comparable with the parental antibody rituximab and were able to bind to both targets with unaltered binding affinity. Notably, our data indicated that CD20-Flex BiFP could not only eliminate lymphoma temporarily but also potentiate tumor-specific T-cell immunity, which affords a long-lasting protection from tumor recurrence. The results showed that the expansion and infiltration of DCs into tumor tissues by CD20-Flex BiFP could be an effective way to generate protective immune responses against cancer, suggesting that the CD20-Flex BiFP could be a promising therapeutic agent against B-cell lymphomas. (*Blood*. 2013;122(26):4230-4236)

## Introduction

Non-Hodgkin lymphoma (NHL) is the fifth most common cancer in the United States and United Kingdom, consisting of indolent and aggressive subtypes with an expected 5 years of overall survival ranging from 25% to 75%.<sup>1,2</sup> The mouse/human chimeric anti-CD20 antibody rituximab is the first therapeutic monoclonal antibodies (mAb) approved for cancer therapy. Though it has revolutionized the management of follicular lymphoma and aggressive B-cell NHL in patients over the past decade, only 48% of patients respond to the treatment, with <10% showing a complete response.<sup>3,4</sup> Increasing evidence shows that several different pathways may contribute to rituximab-mediated tumor suppression, specifically the antibody-dependent cellular cytotoxicity (ADCC), complement-dependent cytotoxicity (CDC), and cell death pathways.<sup>5</sup> However, the in vivo mechanisms of action have yet to be elucidated. Several studies have indicated that maximal clinical and molecular responses to rituximab therapy may take several months, suggesting that short-term cytolytic mechanisms such as cell death, CDC, and ADCC are not the only ones involved.<sup>6</sup> Clinical studies have shown that retreatment with rituximab in patients who had a relapse after an initial response increased the time to progression<sup>7</sup> and that maintenance therapy given to patients in response to rituximab increased the

response rates.<sup>8</sup> Moreover, promising data were recently reported from phase 2 clinical trials where combinations of immunomodulatory cytokines interferon- $\alpha$  or granulocyte-macrophage colony-stimulating factor (GM-CSF) with rituximab for treating B-cell NHL patients produced high clinical response rates and a tolerable safety profile.<sup>9,10</sup> The clinical data suggested that antitumor adaptive immune responses may be elicited in these rituximab therapies and may prolong patient survival.

As expected, several groups have revealed that mechanisms of tumor regression by antibody therapy require adaptive immune responses.<sup>11-13</sup> Additionally, recent studies showed that improvement of effector cell phagocytosis by using CD47 blocking antibody or the direct enhancement of CD8<sup>+</sup> T-cell response through antitumor vaccine substantially increased the therapeutic efficacy of antibody therapy against the cancer.<sup>14,15</sup> Thus, the ideal cancer immunotherapy should increase the influx of both innate and adaptive immune cells into the tumor microenvironment to further enhance subsequent antibody-induced immunity, leading to increased tumor eradication and resistance to rechallenge. Dendritic cells (DCs) are critical for both the induction of primary immune responses and the regulation of T-cell-mediated immune responses.<sup>16</sup> They can conduct all of the

Submitted April 11, 2013; accepted October 27, 2013. Prepublished online as *Blood* First Edition paper, October 31, 2013; DOI 10.1182/blood-2013-04-496554.

L.Z. and Q.T. contributed equally to this work.

The online version of this article contains a data supplement.

The publication costs of this article were defrayed in part by page charge payment. Therefore, and solely to indicate this fact, this article is hereby marked "advertisement" in accordance with 18 USC section 1734.

© 2013 by The American Society of Hematology

elements of the immune orchestra, which are becoming a fundamental target for the induction of protective immunity against cancer and infectious diseases.<sup>17-20</sup> Numerous experimental and clinical studies have indicated that the Flt3 ligand, a hematopoietic growth factor, has the unique ability to dramatically expand the number of both myeloid-related and lymphoid-related DCs<sup>21,22</sup> and could eventually generate protective immune responses against cancer.<sup>23,24</sup> To substantially stimulate antitumor adaptive immunity and consequently provide long-lasting protection against lymphoma, we converted the CD20 antibody rituximab and Flt3-ligand extracellular domain (Flex)-Fc fusion protein into an immunoglobulin (Ig) G-like bispecific protein by using CrossMab technology.<sup>25</sup> Our results indicated that CD20-Flex bispecific fusion protein (BiFP) not only triggers potent CDC, ADCC, and cell death but also efficiently evokes tumor-specific T-cell immunity that could eradicate both human CD20-positive and CD20-shedding lymphoma. More importantly, CD20-Flex BiFP provides long-lasting protection against tumor cells, allowing mice to survive to a subsequent tumor rechallenge. This protective effect was achieved by inducing a cellular immune response that required the presence of both CD4<sup>+</sup> and CD8<sup>+</sup> T cells.

## Materials and methods

### Cell lines, antibodies, and animals

Raji, Daudi, Ramos, RPMI 8226 cells, and A20 cells were obtained from the American Type Culture Collection. A20-CD20 cells were produced by infecting A20 cells with lentiviral virus expressing human CD20 proteins. Fc-deleted CD20-Flex BiFP was generated by thrombin digestion. The secondary antibodies were purchased from Sungene Biotech. SCID mice, BALB/c mice, and Imprinting Control Region mice were housed in specific pathogen-free conditions and treated in accordance with the guidelines of the Committee on Animals of the Second Military Medical University. The study using human peripheral blood mononuclear cells (PBMCs) and hematopoietic progenitor cells (HPCs) from the donors was approved by the Institutional Review Board of the Second Military Medical University. Informed consent from donors was obtained in accordance with the Declaration of Helsinki.

### Binding activity assays

The affinity constant of CD20-Flex BiFP for CD20 and Flt3 receptor was accomplished by radioimmunoassay. The dissociation constants were determined by nonlinear least-squares regression analyses.

### Off-rate measurements

Cells were resuspended in medium with <sup>125</sup>I-labeled BiFP. After 1 hour, cells were resuspended with unlabeled IgG medium. After different time intervals, the samples were analyzed.

### Cytotoxicity assays

After incubation with antibodies for 1 hour, cells were cultured with addition of either normal human serum or human PBMCs. The cell lysis was determined by measuring the amount of lactate dehydrogenase released into the culture supernatant.

### Cell death assay

The cells were incubated with different concentrations of BiFP for 16 hours. After washing, cells were treated with Annexin V-FITC and analyzed by flow cytometry.

### Hematopoiesis assay

Purified HPCs were supplemented with erythropoietin, interleukin-3, and GM-CSF. Total colony numbers were counted on day 14.

### Treatment of established tumors in vivo

Cells were subcutaneously inoculated into the right lateral flank of SCID mice or BALB/c mice separately. When the tumors reached 8 to 10 mm in diameter, antibodies or BiFP were intravenously injected once weekly for 4 doses.

### Assessment of tumor-specific T-cell immunity

After being administered with BiFP or antibodies, the antibody-treated tumor-free mice were rechallenged with A20-CD20 or A20 cells subcutaneously in the opposite flank. Some groups of these mice were intraperitoneally administered with anti-CD4 and/or anti-CD8 mAb after the rechallenge. Effective depletion of CD4<sup>+</sup> and/or CD8<sup>+</sup> T cells was verified by flow cytometry.

### Statistical analysis

Statistical analysis was performed by Student's unpaired *t* test to identify significant differences unless otherwise indicated. Significant differences in tumor incidence at one time point were determined by the Fisher's exact test. Differences were considered significant at a *P* value of <.05.

The detailed procedure can be seen in the supplemental Methods, available on the *Blood* Web site.

## Results

### Design and characterization of CD20-Flex BiFP

Based on CrossMab technology recently reported,<sup>25</sup> we designed an IgG-like bispecific fusion protein (CD20-Flex BiFP) that deviates only minimally from the naturally occurring CD20 antibody rituximab and Flex-Ig. As shown in the right of Figure 1A and supplemental Figure 1A, the constant heavy 1 (CH1) of Flex-CH1-Hinge-CH2-CH3 was replaced with the constant light (CL) of antibody, generating a polypeptide chain made of Flex-CL-Hinge-CH2 and CH3. To generate CD20-Flex BiFP, exchange of CH1 and CL domains in the Flex-CH1-Hinge-CH2-CH3 fragment of the CD20-Flex BiFP is essential for correct association of the light chain and the cognate heavy chain of the half IgG of rituximab in CD20-Flex BiFP. Hetero-dimerization of the rituximab heavy chain and Flex-CL-Hinge-CH2-CH3 was achieved by using the KiH method.<sup>26,27</sup> The resulting highly purified CD20-Flex BiFP was assessed on size-exclusion chromatography (supplemental Figure 1B) and sodium dodecyl sulfate/polyacrylamide gel electrophoresis (supplemental Figure 1C). The stability of CD20-Flex BiFP was also evaluated by incubation of CD20-Flex BiFP in phosphate-buffered saline (PBS) at 37°C for 14 days and subsequent measurement of protein stability through sodium dodecyl sulfate/polyacrylamide gel electrophoresis (supplemental Figure 1D). The binding affinity for CD20 and Flt3 of the CD20-Flex BiFP was determined by analyzing direct cell surface saturation binding to Daudi cells (Figure 1B) and 8266 cells, respectively. The dissociation constant of rituximab (4.83 ± 0.32 nM) is quantitatively consistent with a previous report by Reff et al.<sup>28</sup> It can be seen in Figure 1B that the Fc-deleted CD20-Flex BiFP binding affinity for CD20 (4.82 ± 0.25 nM) is similar to the avidity of rituximab. The similar binding affinity of Flex and CD20-Flex BiFP for Flt3 receptor was also detected (250 ± 20 and 230 ± 40 pmol/L, separately). Additionally, our data showed that Fc-deleted and intact rituximab or BiFP has similar

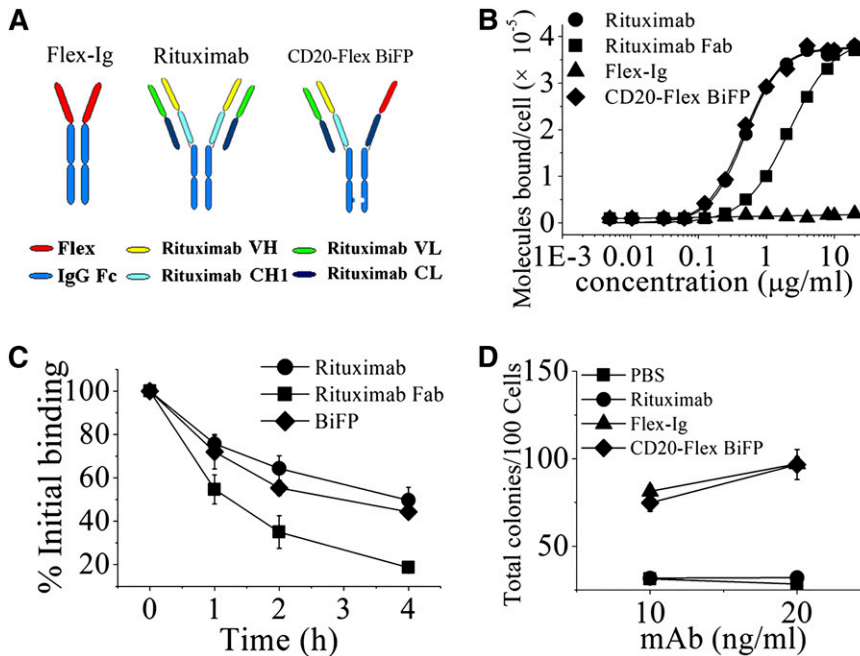


**Figure 1. Characterization of CD20-Flex BiFP.** (A) Schematic diagram of the Fab domain exchange resulting in the generation of CD20-Flex bispecific antibody when combined with the KIH technology. (B) Binding of  $^{125}\text{I}$ -labeled Fc-deleted CD20-Flex BiFP, rituximab  $\text{F(ab')}_2$ , and rituximab Fab fragment to Daudi cells.  $^{125}\text{I}$ -labeled Fc-deleted CD20-Flex BiFP,  $\text{F(ab')}_2$ , or Fab fragments of rituximab were incubated with Daudi cells for 2 h at  $37^\circ\text{C}$ . The saturation of CD20-Flex BiFP is  $\sim 10 \mu\text{g/ml}$ , which is comparable with rituximab. The cell-bound and free  $^{125}\text{I}$ -labeled BiFP or mAb fragments were then separated by centrifugation through phthalate oils and the cell pellets together with bound antibody counted for radioactivity. Data from saturation binding experiments were analyzed by nonlinear least-squares regression for curve-fitting and dissociation constant estimation. Data are mean  $\pm$  SD ( $n = 5$ ). (C) Dissociation of  $^{125}\text{I}$ -labeled CD20-Flex BiFP, rituximab, and rituximab Fab from Raji cells. Cells were incubated with  $^{125}\text{I}$ -labeled CD20-Flex BiFP, rituximab or rituximab Fab ( $10 \mu\text{g/ml}$ ) at  $37^\circ\text{C}$  for 1 h, washed twice, and resuspended. Samples of cells were taken at time 0, 1, 2, and 4 hours and then washed and analyzed. Shown are means and SD of at least 3 experiments. (D) Validated Flex function of CD20-Flex BiFP. Both Flex-Ig and CD20-Flex BiFP exhibited dose-response curves (10 and 20 ng/mL) for purified HPC colonies, as evaluated in cultures supplemented with 2 U/mL erythropoietin, 10 ng/mL interleukin-3, 20 ng/mL GM-CSF. Mean  $\pm$  SD values from 4 separate experiments.

binding activities (data not shown). These data indicated that CD20-Flex BiFP keep the intact affinity bound to CD20 and Fc $\gamma$ 3.

Binding “off-rate” experiments using  $^{125}\text{I}$ -labeled IgG were performed to compare the dissociation of rituximab and CD20-Flex BiFP from Raji cells. As shown in Figure 1C, the data showed a slight difference in the off-rate between CD20-Flex BiFP and rituximab. Approximately 60% of the rituximab, and more than 54% of CD20-Flex BiFP, remained bound to the cells after 2 hours. In addition, similar results were achieved with  $\text{F(ab')}_2$ , which excluded an interaction with Fc $\gamma$ R on target cells influencing mAb dissociation (data not shown). To investigate the intact function of Flex in the CD20-Flex BiFP, we evaluated the effect of CD20-Flex BiFP on the number of colonies generated by purified HPCs. Our data showed that Flex-Ig or CD20-Flex BiFP (10 or 20 ng/mL) in combination with saturating concentrations of interleukin-3, GM-

CSF, and erythropoietin elicited a dose-dependent increase in the total colony number (Figure 1D). Compared with the parental antibody rituximab and fusion protein Flex-Ig, the data indicated that CD20-Flex BiFP had similar binding activity and functions.

#### CD20-Flex BiFP effectively induces antitumor activity as comparable with rituximab

In initial functional experiments, the cytotoxic activities of CD20-Flex BiFP were assessed against 2 CD20 $^+$  human lymphoma cell lines, Daudi and Raji. In line with our expectations, BiFP displayed approximately the same level of CDC activity as rituximab (Figure 2A-B). To determine the BiFP-mediated ADCC by PBMCs, a standard lactate dehydrogenase assay was performed. Purified human PBMCs from healthy donors were used as effector cells and Daudi cells were used as

**Figure 2. The in vitro antitumor effects of CD20-Flex BiFP against lymphoma.** Raji (A) and Daudi (B) cells were incubated with increasing concentrations of CD20 antibodies and Flex-Ig fusion protein in the presence of human complement at  $37^\circ\text{C}$  for 4 h. CDC activity was calculated by a standard lactate dehydrogenase assay as described in “Materials and methods.” These graphs are representative of at least 3 experiments, each showing similar results. (C) ADCC activity against Daudi cells using human PBMCs as effector cells at an effector-to-target cell (E:T) ratio of 25:1. The ADCC activity of CD20-Flex BiFP at varying concentrations was measured using a standard lactate dehydrogenase assay as described in “Materials and methods.” Data are expressed as means  $\pm$  SD ( $n = 3$ ). (D) Inhibition of CD20 antibody-induced cell death by ZVAD. Before Raji cells were incubated with 10  $\mu\text{g/ml}$  rituximab or CD20-Flex BiFP in the presence of cross-linker (x-link, goat anti-human  $\kappa$   $\text{F(ab')}_2$  fragment, 20  $\mu\text{g/ml}$ ), caspase inhibitor ZVAD was added over a range of different concentrations for 2 hours. Shown are means and SD of at least 3 experiments.

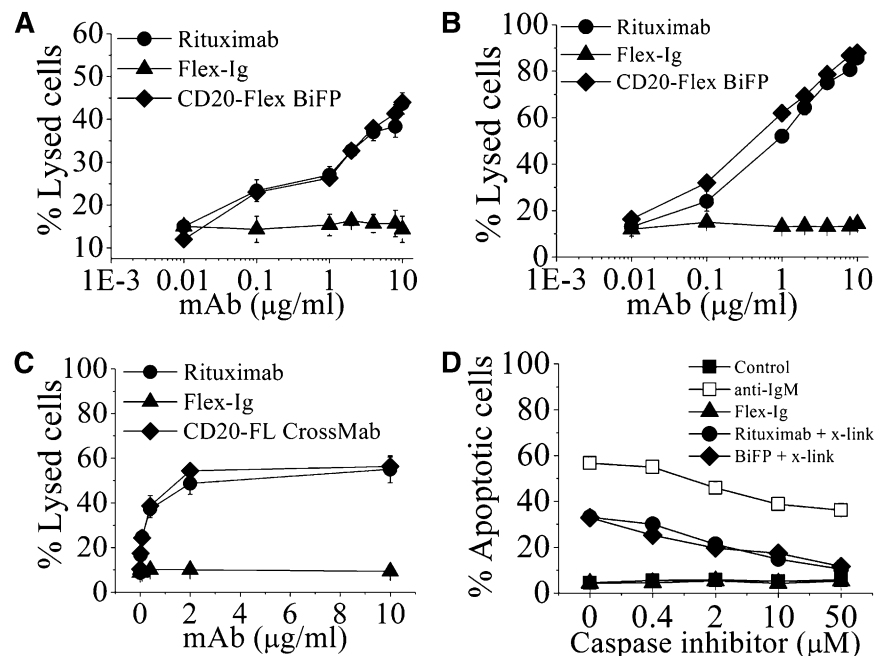
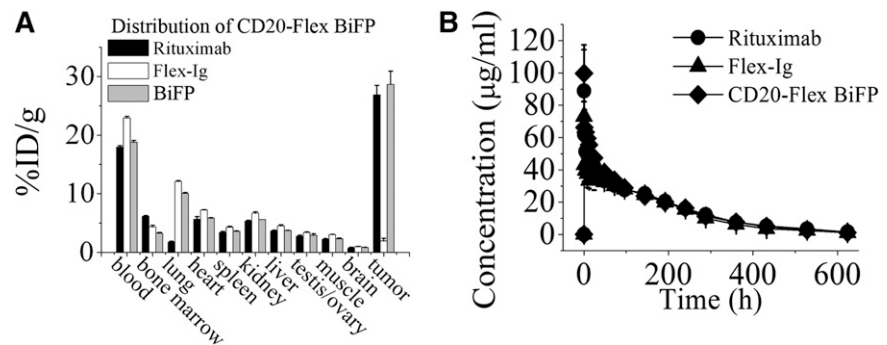


**Figure 3. Distribution and pharmacokinetic of CD20-Flex BiFP.** (A) The distribution of CD20-Flex BiFP. BALB/c mice bearing A20-CD20 tumors were intravenously injected with 0.1 mL ( $2 \times 10^6$  counts per minute/mouse) of  $^{125}\text{I}$ -labeled rituximab, Flex-Ig, or CD20-Flex BiFP. At 24 hours after injection, the animals were sacrificed and different tissue samples were collected and assayed for radioactivity. Data are presented as %ID/g of tissue and values are the mean  $\pm$  SD derived from 3 organs of 3 different animals. (B) Groups of 8-week-old female Inprinting Control Region mice were injected with 10 mg/kg rituximab, Flex-Ig, or CD20-Flex BiFP via the tail vein. Antibody concentrations in plasma were determined. Each data point is the mean  $\pm$  SD of the measurements of 3 samples from 3 different animals.



the target. Assays were conducted at E:T ratios of 25:1 using antibody concentrations ranging from 0.003 to 10  $\mu\text{g}/\text{mL}$  (Figure 2C). To facilitate a comparative analysis of the data, we evaluated the concentrations of antibody needed for 50% cytotoxicity at E:T ratios of 25:1. Our data showed that 2  $\mu\text{g}/\text{mL}$  of rituximab or BiFP was required to achieve the targeted lysis levels. Similar results were also obtained with Raji cells (data not shown). Subsequently, induction of cell death was evaluated by FITC-Annexin V assays in Raji cells. As indicated in Figure 2D, after they were cross-linked with anti-human  $\kappa$  F(ab')<sub>2</sub> fragment, BiFP and rituximab triggered a similar level of cell death (>30%) in Raji cells at the concentration of 10  $\mu\text{g}/\text{mL}$ . When adding cell-permeable caspase inhibitor N-Benzyloxycarbonyl-Val-Ala-Asp(O-Me) fluoromethyl ketone (ZVAD-FMK) in the range from 0.4 to 50  $\mu\text{M}$ , our experimental results revealed ZVAD-FMK was able to prevent both CD20-Flex BiFP- and rituximab-induced cell death in the presence of cross-linker (Figure 2D). Further studies showed that both CD20-Flex BiFP and rituximab could not induce significant lysosome membrane permeabilization and cathepsin release. The cross-linking-induced cell death triggered by BiFP or rituximab cannot be inhibited by cathepsin inhibitor (data not shown). These results demonstrated that CD20-Flex BiFP could efficiently trigger potent CDC, ADCC, and cell death as comparable with rituximab.

#### Tissue distributions and pharmacokinetics of CD20-Flex BiFP in mice

To further assess if conversion of rituximab to CD20-Flex BiFP altered the in vivo antibody behavior, we compared the tissue distribution of CD20-Flex BiFP with that of rituximab. Three separate groups of mice were treated with  $^{125}\text{I}$ -labeled rituximab,  $^{125}\text{I}$ -labeled Flex-Ig, or  $^{125}\text{I}$ -labeled CD20-Flex BiFP via tail vein injections. At 24 hours after the administration, the animals in each group were killed and exsanguinated by flushing the circulatory system with PBS. The organs were then removed, weighed, and assayed for  $^{125}\text{I}$  radioactivity. The percent of injected dose per gram of tissue (%ID/g) was calculated for each animal. The mean values were calculated and are graphically presented in Figure 3A. A comparison of the data showed no significant observable differences between rituximab and CD20-Flex BiFP for the tissue localization. Both rituximab and BiFP were largely present in the tumor site and blood compartments. Furthermore, the kinetics of tumor clearance of  $^{125}\text{I}$ -labeled rituximab, Flex-Ig, or CD20-Flex BiFP in tumor-bearing BALB/c mice were analyzed (supplemental Figure 2). Rituximab showed continuous accumulation, reaching 34.3%ID/g at 72 hours. Compared with rituximab, CD20-Flex BiFP also accumulated in the tumor at a comparable level to reach a maximum of 36.3%ID/g after 72 hours.

BALB/c mice were intravenously injected with the same amount of rituximab, Flex-Ig, or CD20-Flex BiFP. Blood samples were

withdrawn at different time points over a period of 26 days to assay the protein concentrations in the whole blood. The data are shown in Figure 3B, where the blood concentrations of rituximab, Flex-Ig, and BiFP, as determined using the ELISA method, are plotted against the time of sampling in hours after administration. The pharmacokinetic variables were calculated using a noncompartmental analysis. The terminal half-life periods of CD20-Flex BiFP, rituximab, and Flex-Ig were 102, 114, and 100 hours, respectively (Figure 3B).

#### Long-lasting antitumor protection by CD20-Flex BiFP against B-cell lymphoma

To determine whether initial CD20-Flex BiFP therapy induces an antitumor response that can protect mice after tumor challenge, we subcutaneously injected  $5 \times 10^6$  Daudi cells into SCID mice on day 0. When the tumors reached 8 to 10 mm in diameter, 10 mg/kg rituximab, Flex-Ig, CD20-Flex BiFP, or rituximab and Flex-Ig was intravenously injected once weekly for 4 doses. As shown in Figure 4A and supplemental Figure 5, although all of the treatments can induce the complete rejection of established (80 mm<sup>2</sup>) subcutaneous Daudi cells in mice ( $P < .001$  for each compared with the PBS control), the suboptimal doses of CD20-Flex BiFP exhibited more potent antitumor efficacy than that of rituximab ( $P < .05$  compared with the rituximab-treated group). To further explore the long-lasting antitumor activity of CD20-Flex BiFP, we first transfected human CD20 into murine B-cell lymphoma A20 cells to establish A20-CD20 mouse model as previously described.<sup>29,30</sup> CD20 expression levels were measured by mean fluorescence intensity. As illustrated in supplemental Figure 6A, A20-CD20 cells showed similar CD20 surface expression compared with Ramos cells, whereas human CD20 expression was not detectable on the plasma membrane of A20 cells. Similar to human B-cell lymphoma, CDC, ADCC, and cross-linking-induced cell death could be detected in A20-CD20 cells after treatment with rituximab or CD20-Flex BiFP (supplemental Figure 6B-D). After complete rejection of low doses of A20-CD20 cells in wild-type BALB/c mice by treatment with rituximab, Flex-Ig, BiFP, or rituximab and Flex-Ig, the mice were rechallenged with A20-CD20 or A20 cells on the opposite flank. Surprisingly, our data showed that only the CD20-Flex BiFP-treated group significantly rejected A20-CD20 cells ( $P < .01$ ), although some suppression of tumor growth was still observed in the rituximab-, Flex-Ig-, and rituximab and Flex-Ig-treated groups (Figure 4B-C). The most striking finding in our present study was that the BiFP-treated group still exhibited the capacity to cause substantial regression of A20 tumors (Figure 4D;  $P < .01$ ), which normally do not express human CD20 surface protein. These results indicated that CD20-Flex BiFP could trigger long-lasting antitumor protection against both CD20 positive and CD20 negative lymphoma, suggested that antitumor immune responses may be critical for long-lasting antitumor protection initiated by BiFP.



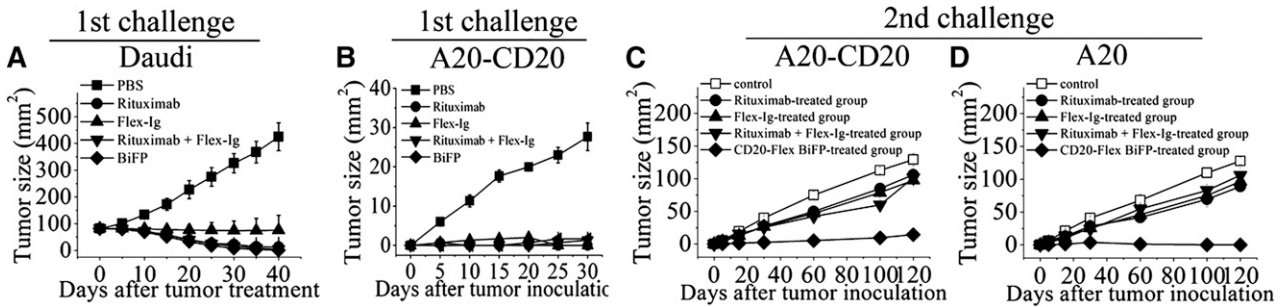


**Figure 4. In vivo antitumor activity of CD20-Flex BiFP.** (A) Groups of SCID mice were subcutaneously inoculated with  $5 \times 10^6$  Daudi. When the tumors reached 8 to 10 mm in diameter, 10 mg/kg rituximab, Flex-Ig, CD20-Flex BiFP, or PBS was intravenously injected once weekly for 4 doses. Tumor size was measured 2-dimensionally with a caliper. (B-D) BALB/c mice were inoculated with A20-CD20 cells and then treated with rituximab, Flex-Ig, CD20-Flex BiFP, or rituximab combined with Flex-Ig ( $n = 25$ ) (B). The antibody-treated tumor-free mice were then rechallenged with A20-CD20 (C) or A20 cells (D) subcutaneously in the opposite flank on day 42 (solid symbols). Naive mice were inoculated with A20-CD20 cells (middle) or A20 cells (right) as the control. The primary tumor material is examined through measurement of tumor size and IHC analysis. The graphs are representative of at least 5 experiments, each of which showed similar results.

**Induction of tumor-specific T-cell immunity by BiFP-mediated tumor rejection**

To evaluate the contribution of antitumor immunity for BiFP-induced long-lasting protection, the infiltrating immune cells, including NK, DC,  $CD4^+$  T cells, and  $CD8^+$  T cells, were first assessed in the treated tumors site up to 8 days after BiFP treatment. As illustrated in Figure 5, significantly larger numbers of infiltrating DC and  $CD8^+$  T cells were observed at the tumor site in the BiFP-treated mice compared with the control Ig-treated mice ( $P < .01$ ). However, a marked difference in infiltration of DC or  $CD8^+$  T cells was not observed after rituximab or Flex-Ig treatment. To further investigate the role of DC in the promotion of tumor-specific T-cell immunity, we first analyzed the kinetics of generation of DCs in spleen and peripheral blood after treatment with BiFP. The absolute number of DCs was markedly increased in both spleen and peripheral blood after 10 days (supplemental Figure 3;  $P < .01$  compared with control group). Further studies showed that depletion of DCs through diphtheria toxin injection significantly influence the tumor-specific T-cell immunity triggered by CD20-Flex BiFP (supplemental Figure 4). Subsequently, we examined whether eradication of primary A20-CD20 tumors by CD20-Flex BiFP treatment enabled the induction of tumor-specific T-cell immunity. Administration of BiFP resulted in complete rejection of  $10^4$  A20-CD20 cells in BALB/c mice (Figure 6A, left). When rechallenged with A20-CD20 cells on the opposite flank, these mice rejected A20-CD20 cells (Figure 6A, middle). Depletion of either

$CD8^+$  T cells or  $CD4^+$  T cells abrogated the secondary rejection, although some suppression of tumor growth was still observed in the  $CD4^+$  T-cell-depleted mice (Figure 6A, middle). To further validate the tumor-specific immune response, irrelevant 4T1 tumor cells were inoculated into A20-CD20-rejecting mice or naive mice. No obvious differences were observed, indicating that BALB/c mice preimmunized with A20-CD20 cells did not reject the secondary challenge with irrelevant 4T1 tumor cells (Figure 6A, right). Moreover, adoptive transfer of splenic T cells isolated from A20-CD20 rejecting BALB/c mice ( $P < .01$ ), but not those isolated from naive BALB/c mice, protected SCID mice from a lethal dose of A20-CD20 tumor challenge (Figure 6B, right). These results indicated that CD20-Flex BiFP could elicit tumor-specific T-cell immunity against B-cell lymphoma.

**Discussion**

In our present study, we successfully converted therapeutic antibody rituximab and Flex-Ig into a bispecific IgG-like protein by using CrossMab technology as previously described.<sup>25</sup> Our data showed that the bispecific CD20-Flex BiFP exhibited a stability comparable with its parental antibodies and bound CD20 and Flt3 receptor with affinity similar to that of rituximab and Flt3 ligand. As we know, the classical IgG architecture as it was selected during evolution has

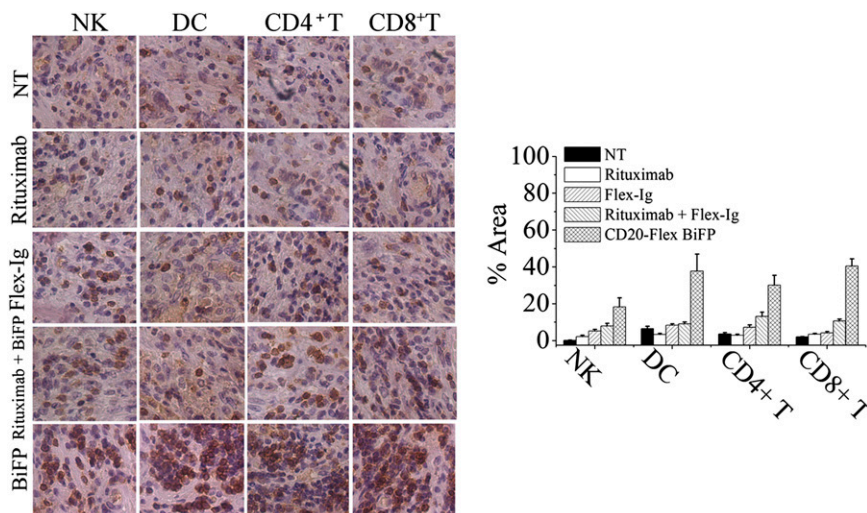
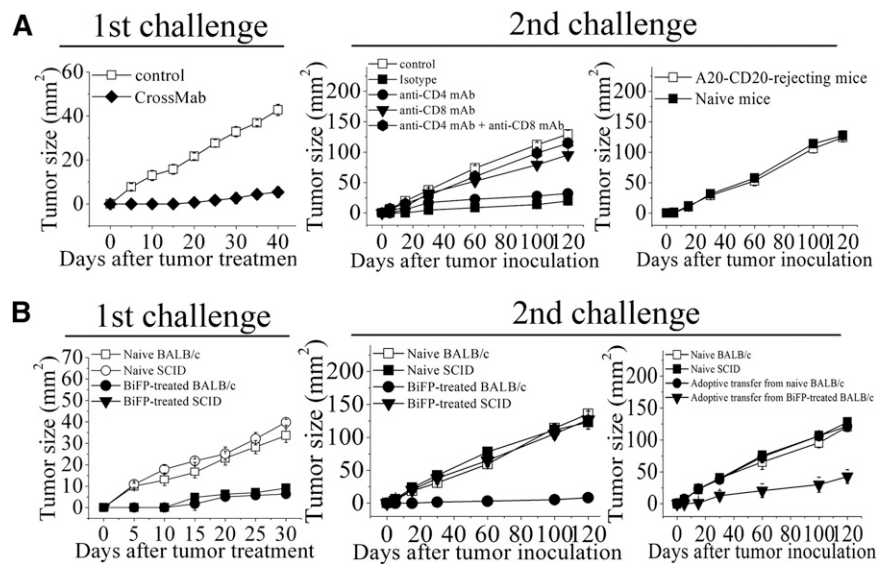


**Figure 5. CD20-Flex BiFP induces infiltration of DCs and  $CD8^+$  T cells in tumor site.** Tumor was removed 8 days after tumor inoculation from control Ig-, rituximab-, Flex-Ig-, or CD20-Flex BiFP-treated mice and then were embedded in Tissue-Tek OCT compound and frozen in liquid nitrogen. Tissues were sectioned on a cryostat.  $CD56^+$  NK cells,  $CD11c^+$  DC,  $CD4^+$  T cells, and  $CD8^+$  T cells were stained by a routine IHC protocol. Representative of 5 tumors in each group. Quantification of IHC images using the NIH ImageJ software package. The values are indicated as percent area in comparison with the staining obtained from the NT group.

**Figure 6. Induction of tumor-specific T-cell memory by BiFP-mediated tumor rejection.** (A) BALB/c mice were subcutaneously inoculated with A20-CD20 cells and then treated with CD20-Flex BiFP or control Ig (left). After the first inoculation, the BiFP-treated mice were secondarily inoculated with A20-CD20 cells. Some mice were treated with anti-CD4 mAb, anti-CD8 mAb, anti-CD4, and anti-CD8 mAb or isotype Ig (middle). Naive mice were inoculated with A20-CD20 cells as the control. Irrelevant 4T1 tumor cells were inoculated into A20-CD20–rejecting mice or naive mice (right). (B) BALB/c and SCID mice were inoculated with A20-CD20 cells and then treated with CD20-Flex BiFP mAb (200  $\mu$ g) ( $n = 25$ ; 800  $\mu$ g) or control Ig ( $n = 25$ ) (left). Five weeks after the first inoculation, the BiFP-treated BALB/c and SCID mice that had rejected A20-CD20 were secondarily inoculated with A20-CD20 cells (middle). Naive BALB/c and SCID mice were inoculated with A20-CD20 cells as the control. Two days after inoculation of A20-CD20 cells, some SCID mice were intravenously transferred with splenic T cells from the BiFP-treated BALB/c mice that had rejected A20-CD20 or naive BALB/c mice (right). Naive SCID mice and naive BALB/c mice as the control. The graphs are representative of at least 5 experiments, each of which showed similar results.



many advantages for therapeutic application.<sup>31</sup> The Fc part is identical to that of a conventional IgG antibody, resulting in IgG-like pharmacokinetic properties and retained effector functions such as the mediation of ADCC through Fc $\gamma$ RIIIa binding. IgG-like size and molecular weight are expected to result in IgG-like diffusion, tumor penetration, and accumulation in comparison with bispecific tetravalent antibodies of higher molecular weight. The antibody-Flex cross-over approach leaves the antigen-binding regions of the parental antibody and fusion protein intact; the method provides a way to convert any therapeutic antibodies and fusion protein into an almost natural bispecific IgG-like BiFP. Additionally, a bispecific CD20-Flex BiFP protein generated in this study could be expressed using a conventional transient antibody expression system comparable in yields and quality with conventional IgG antibodies and could be purified using standard IgG purification procedures. All these benefits of BiFP indicated that it has strong potential as a therapeutic agent for cancer treatment.<sup>32,33</sup>

Recent studies revealed that the *in vivo* mechanisms of tumor regression by both anti-HER2/neu and anti-CD20 antibody therapy require adaptive immune responses.<sup>11,34</sup> In accordance with their findings, our experimental data showed that, after rechallenge with A20-CD20 cells or A20 cells, some suppression of tumor growth was observed in rituximab- and Flex-Ig–treated groups, suggesting that treatment with rituximab or Flex-Ig alone does not trigger a sufficient level of adaptive immune response against tumors (supplemental Figure 5). Further studies showed that significantly larger numbers of infiltrating DC and CD8<sup>+</sup> T cells at the tumor site were not observed after treatment with rituximab or Flex-Ig. It is worthy to note that even in the rituximab combined with Flex-Ig treatment group, the significant inhibition of tumor growth, after the secondary tumor inoculation, was not found. In contrast, we observed that BiFP induced infiltration of large numbers of DC and CD8<sup>+</sup> T cells into the tumor site and consequently produced a marked rejection of rechallenged A20-CD20 cells in CD20-Flex BiFP-treated mice. Our data revealed that CD20-Flex BiFP has the ability to induce infiltration of DC and CD8<sup>+</sup> T cells into the tumor site, which might be critical for eliciting the antitumor immune response for long-lasting protection.

Emergence of rituximab resistance is a critical problem for rituximab-based therapy. A number of impressive clinical studies

have recently revealed that down-regulation of CD20 on the plasma membrane after treatment with rituximab limits the therapeutic efficacy of CD20 antibody therapy.<sup>35–39</sup> Their data showed that internalization of CD20 triggered by rituximab led to reduced macrophage recruitment and the degradation of CD20/mAb complexes, shortening mAb half-life. Moreover, most cases of chronic lymphatic leukemia and mantle cell lymphoma showed rapid CD20 internalization after rituximab treatment.<sup>35,40,41</sup> Although the mechanism of rituximab resistance in B-cell lymphoma remains unclear, CD20 shedding may be partially responsible for the resistance to rituximab treatment.<sup>42,43</sup> Our results showed that the long-lasting antitumor protection initiated by CD20-Flex BiFP treatment can also protect mice from a subsequent tumor challenge with no human CD20-expressing A20 cell lines. The tumor-specific T-cell immunity has been further validated by the rechallenge of irrelevant 4T1 tumor cells and depletion of DC, CD8<sup>+</sup> T cells, and CD4<sup>+</sup> T cells during the secondary tumor inoculation. Although the respective contribution of CDC, ADCC, and cell death induced by BiFP need to be further illustrated, our results indicated that induction of antitumor T-cell immunity by CD20-Flex BiFP provided long-term tumor-specific protection against both human CD20<sup>+</sup> and human CD20<sup>–</sup> lymphoma, suggesting that CD20-Flex BiFP may have the potential to become a promising agent to overcome resistance on long-term rituximab therapy. As we known, syngeneic tumor models may not fully represent the complexity of human tumors in clinical situations.<sup>44</sup> Spontaneous tumor models provide unique insight into tumor development. We are developing spontaneous B-cell lymphoma models in an attempt to further investigate the relationship between tumor-specific T-cell immunity and antitumor activity of CD20-Flex BiFP.

In conclusion, the bispecific IgG-like CD20-Flex BiFP therapy might be an efficient strategy not only to eliminate rituximab-sensitive lymphoma temporarily, but also to potentiate tumor-specific T-cell immunity that affords a long-term protection from tumor recurrence.

## Acknowledgments

This work was supported by grants from the National Natural Science Foundation of China, Ministry of Science and Technology of China

(973 and 863 program projects), National Key Project for New Drug Creation and Manufacture, and Shanghai Commission of Science and Technology, Shanghai Leading Academic Discipline Project, and Program for Innovative Research Team in University.

## Authorship

Contribution: Y.G., S.H., and L.Z. designed research, analyzed data, and wrote the manuscript; and Q.T., B.L., W.Q., D.Z., T.F.,

S.D., X.Z., J.Z., J.D., and H.W. performed experiments and analyzed data.

Conflict-of-interest disclosure: The authors declare no competing financial interests.

Correspondence: Yajun Guo, International Joint Cancer Institute and PLA General Hospital Cancer Center, New Library Building, 10-11th floor, 800 Xiang Yin Rd, Shanghai 200433, P.R. China; e-mail: yjguo@smmu.edu.cn; and Sheng Hou, International Joint Cancer Institute and PLA General Hospital Cancer Center, New Library Building 10-11th floor, 800 Xiang Yin Rd, Shanghai 200433, P.R. China; e-mail: housheng301@163.com.

## References

- Shankland KR, Armitage JO, Hancock BW. Non-Hodgkin lymphoma. *Lancet*. 2012;380(9844):848-857.
- Hennessy BT, Hanrahan EO, Daly PA. Non-Hodgkin lymphoma: an update. *Lancet Oncol*. 2004;5(6):341-353.
- Calcagno A, Rostagno R, Di Perri G. Anti-CD20 antibody therapy for B-cell lymphomas. *N Engl J Med*. 2012;367(9):877-878, author reply 878.
- Boye J, Elter T, Engert A. An overview of the current clinical use of the anti-CD20 monoclonal antibody rituximab. *Ann Oncol*. 2003;14(4):520-535.
- Glennie MJ, French RR, Cragg MS, Taylor RP. Mechanisms of killing by anti-CD20 monoclonal antibodies. *Mol Immunol*. 2007;44(16):3823-3837.
- Cartron G, Watier H, Golay J, Solal-Celigny P. From the bench to the bedside: ways to improve rituximab efficacy. *Blood*. 2004;104(9):2635-2642.
- Davis TA, Grillo-López AJ, White CA, et al. Rituximab anti-CD20 monoclonal antibody therapy in non-Hodgkin's lymphoma: safety and efficacy of re-treatment. *J Clin Oncol*. 2000;18(17):3135-3143.
- Hainsworth JD, Litchy S, Burris HA III, et al. Rituximab as first-line and maintenance therapy for patients with indolent non-hodgkin's lymphoma. *J Clin Oncol*. 2002;20(20):4261-4267.
- Kimby E, Jurlander J, Geisler C, et al; Nordic Lymphoma Group. Long-term molecular remissions in patients with indolent lymphoma treated with rituximab as a single agent or in combination with interferon alpha-2a: a randomized phase II study from the Nordic Lymphoma Group. *Leuk Lymphoma*. 2008;49(1):102-112.
- Cartron G, Zhao-Yang L, Baudard M, et al. Granulocyte-macrophage colony-stimulating factor potentiates rituximab in patients with relapsed follicular lymphoma: results of a phase II study. *J Clin Oncol*. 2008;26(16):2725-2731.
- Park S, Jiang Z, Mortenson ED, et al. The therapeutic effect of anti-HER2/neu antibody depends on both innate and adaptive immunity. *Cancer Cell*. 2010;18(2):160-170.
- Uno T, Takeda K, Kojima Y, et al. Eradication of established tumors in mice by a combination antibody-based therapy. *Nat Med*. 2006;12(6):693-698.
- Takeda K, Yamaguchi N, Akiba H, et al. Induction of tumor-specific T cell immunity by anti-DR5 antibody therapy. *J Exp Med*. 2004;199(4):437-448.
- Chao MP, Alizadeh AA, Tang C, et al. Anti-CD47 antibody synergizes with rituximab to promote phagocytosis and eradicate non-Hodgkin lymphoma. *Cell*. 2010;142(5):699-713.
- Kim PS, Armstrong TD, Song H, et al. Antibody association with HER-2/neu-targeted vaccine enhances CD8 T cell responses in mice through Fc-mediated activation of DCs. *J Clin Invest*. 2008;118(5):1700-1711.
- Palucka K, Banchereau J. Cancer immunotherapy via dendritic cells. *Nat Rev Cancer*. 2012;12(4):265-277.
- Banchereau J, Brière F, Caux C, et al. Immunobiology of dendritic cells. *Annu Rev Immunol*. 2000;18:767-811.
- Banchereau J, Palucka AK. Dendritic cells as therapeutic vaccines against cancer. *Nat Rev Immunol*. 2005;5(4):296-306.
- Mellman I, Coukos G, Dranoff G. Cancer immunotherapy comes of age. *Nature*. 2011;480(7378):480-489.
- Mocikat R, Braumüller H, Gumy A, et al. Natural killer cells activated by MHC class I(low) targets prime dendritic cells to induce protective CD8 T cell responses. *Immunity*. 2003;19(4):561-569.
- Maraskovsky E, Daro E, Roux E, et al. In vivo generation of human dendritic cell subsets by Flt3 ligand. *Blood*. 2000;96(3):878-884.
- Maraskovsky E, Brasel K, Teepe M, et al. Dramatic increase in the numbers of functionally mature dendritic cells in Flt3 ligand-treated mice: multiple dendritic cell subpopulations identified. *J Exp Med*. 1996;184(5):1953-1962.
- Fong L, Hou Y, Rivas A, et al. Altered peptide ligand vaccination with Flt3 ligand expanded dendritic cells for tumor immunotherapy. *Proc Natl Acad Sci USA*. 2001;98(15):8809-8814.
- Lynch DH, Andreassen A, Maraskovsky E, Whitmore J, Miller RE, Schuh JC. Flt3 ligand induces tumor regression and antitumor immune responses in vivo. *Nat Med*. 1997;3(6):625-631.
- Schaefer WW, Regula J, Böhner MM, et al. Immunoglobulin domain crossover as a generic approach for the production of bispecific IgG antibodies. *Proc Natl Acad Sci USA*. 2011;108(27):11187-11192.
- Atwell SS, Ridgway J, Wells J, Carter PP. Stable heterodimers from remodeling the domain interface of a homodimer using a phage display library. *J Mol Biol*. 1997;270(1):26-35.
- Ridgway JB, Presta LG, Carter P. 'Knobs-into-holes' engineering of antibody CH3 domains for heavy chain heterodimerization. *Protein Eng*. 1996;9(7):617-621.
- Reff ME, Carner K, Chambers KS, et al. Depletion of B cells in vivo by a chimeric mouse human monoclonal antibody to CD20. *Blood*. 1994;83(2):435-445.
- Minard-Colin V, Xiu Y, Poe JC, et al. Lymphoma depletion during CD20 immunotherapy in mice is mediated by macrophage FcγRI, FcγRIII, and FcγRIV. *Blood*. 2008;112(4):1205-1213.
- Olafsen T, Betting D, Kenanova VE, et al. Recombinant anti-CD20 antibody fragments for small-animal PET imaging of B-cell lymphomas. *J Nucl Med*. 2009;50(9):1500-1508.
- Scott AM, Wolchok JD, Old LJ. Antibody therapy of cancer. *Nat Rev Cancer*. 2012;12(4):278-287.
- Chames P, Baty D. Bispecific antibodies for cancer therapy: the light at the end of the tunnel? *MAbs*. 2009;1(6):539-547.
- Beck A, Wurch T, Bailly C, Corvaia N. Strategies and challenges for the next generation of therapeutic antibodies. *Nat Rev Immunol*. 2010;10(5):345-352.
- Abès R, Gélizé E, Fridman WH, Teillaud J-L. Long-lasting antitumor protection by anti-CD20 antibody through cellular immune response. *Blood*. 2010;116(6):926-934.
- Beers SA, French RR, Chan HT, et al. Antigenic modulation limits the efficacy of anti-CD20 antibodies: implications for antibody selection. *Blood*. 2010;115(25):5191-5201.
- Hiraga J, Tomita A, Sugimoto T, et al. Down-regulation of CD20 expression in B-cell lymphoma cells after treatment with rituximab-containing combination chemotherapies: its prevalence and clinical significance. *Blood*. 2009;113(20):4885-4893.
- Jilani I, O'Brien S, Manshuri T, et al. Transient down-modulation of CD20 by rituximab in patients with chronic lymphocytic leukemia. *Blood*. 2003;102(10):3514-3520.
- Beum PV, Lindorfer MA, Taylor RP. Within peripheral blood mononuclear cells, antibody-dependent cellular cytotoxicity of rituximab-opsonized Daudi cells is promoted by NK cells and inhibited by monocytes due to shaving. *J Immunol*. 2008;181(4):2916-2924.
- Beum PV, Peek EM, Lindorfer MA, et al. Loss of CD20 and bound CD20 antibody from opsonized B cells occurs more rapidly because of trogocytosis mediated by Fc receptor-expressing effector cells than direct internalization by the B cells. *J Immunol*. 2011;187(6):3438-3447.
- Manshoury T, Do K-A, Wang X, et al. Circulating CD20 is detectable in the plasma of patients with chronic lymphocytic leukemia and is of prognostic significance. *Blood*. 2003;101(7):2507-2513.
- Kennedy AD, Beum PV, Solga MD, et al. Rituximab infusion promotes rapid complement depletion and acute CD20 loss in chronic lymphocytic leukemia. *J Immunol*. 2004;172(5):3280-3288.
- Czuczman MS, Olejniczak S, Gowda A, et al. Acquisition of rituximab resistance in lymphoma cell lines is associated with both global CD20 gene and protein down-regulation regulated at the pretranscriptional and posttranscriptional levels. *Clin Cancer Res*. 2008;14(5):1561-1570.
- Taylor RP, Lindorfer MA. Antigenic modulation and rituximab resistance. *Semin Hematol*. 2010;47(2):124-132.
- Teicher BA. Tumor models for efficacy determination. *Mol Cancer Ther*. 2006;5(10):2435-2443.